High-Temperature Low-Cycle Fatigue Behavior of Superalloy MA 760

A. Hynnä, V.-T. Kuokkala, J. Laurila, and P. Kettunen

The high-temperature cyclic behavior of oxide dispersion-strengthened superalloy MA 760 was studied at different temperatures and specimen orientations. The cyclic hardening curves at different strain amplitudes were determined at 650, 900, and 950 °C, and the stress-strain response of the material was substantiated by detailed fractographical scanning electron microscopy (SEM) and microstructural/optical microscopy, STEM) observations. During cycling, MA 760 did not exhibit marked hardening or softening, and also the final fracture occurred very rapidly without a significant decrease in the cyclic strength of the material. The "brittle" nature of deformation behavior of MA 760, especially at lower test temperatures, as well as oxidation-induced secondary cracking along grain boundaries, was clearly revealed by microscopical studies of the fracture surfaces. At 650 °C, evidence of dislocation cutting of γ′ was observed in transmission micrographs, but at higher temperatures, dislocation climb and by-passing of γ′ particles were found to become more prominent features. At all test temperatures, dislocation climb over yttria particles, as well as the departure side pinning effect of dislocations at nonshearable particles, was frequently observed.

Keywords
fatigue, high-temperature low-cycle fatigue, superalloys: MA 760

1. Introduction

OXIDE dispersion-strengthened (ODS) superalloys form one of the new material groups developed in search for materials with improved properties in extreme operating conditions. They maintain their high strength and good corrosion resistance at higher temperatures than conventional superalloys and are therefore of great interest, for example, to designers of gas turbine engines.[1] These ODS superalloys are produced by mechanical alloying process,[2] followed, e.g., by extrusion, hot rolling, recrystallization, and γ′ precipitation heat treatments. The excellent properties of ODS alloys are due to the very fine dispersion of stable incoherent oxide particles, formed during the mechanical alloying process, which act as barriers to the movement of dislocation.[3] Nickel-base ODS superalloys can also be strengthened by coherent γ′ precipitates. The γ′ strengthening is active at lower temperatures than dispersion strengthening, which becomes dominant at temperatures above 1000 °C.[4] After recrystallization heat treatment, the grain structure of ODS alloys is very coarse, and the grain aspect ratio (GAR) is large. Together with highly serrated grain boundaries, these properties are beneficial in high-temperature service, where the amount of transverse grain boundaries should be minimized.[5]

The creep and fatigue properties of ODS superalloys have been studied intensively during the past few years, but the existing data are still incomplete. This is especially true for MA 760, a modified more corrosion-resistant version of the well-known MA 6000. In this article, the low-cycle fatigue (LCF) properties of MA 760 at 650, 900, and 950 °C are reported, together with fractographical (SEM) and microstructural (STEM) observations.

A. Hynnä, V.-T. Kuokkala, and **P. Kettunen,** Tampere University of Technology, Institute of Materials Science; and **J. Laurila,** Research Center for Materials Science, P.O. Box 589, SF-33101 Tampere, Finland.

Table 1 Composition of test materials

Element	Composition, wt%
Large cross section specimen	
Cr	19.79
Al	5.93
Mo	1.96
W	3.5
Fe	1.04
C	0.042
Zr	0.14
N	0.286
S	0.003
P	<0.005
B	0.11
Y_2O_3	1.03
Si	0.04
O	0.60
Small cross section specimen	
Cr	19.66
Al	5.97
Mo	1.92
W	3.5
Fe	1.02
C	0.043
Zr	0.14
N	0.284
S	0.003
P	<0.005
B	0.11
Y_2O_3	1.03
Si	0.04
O	0.54
Co	0.05
Ti	0.02

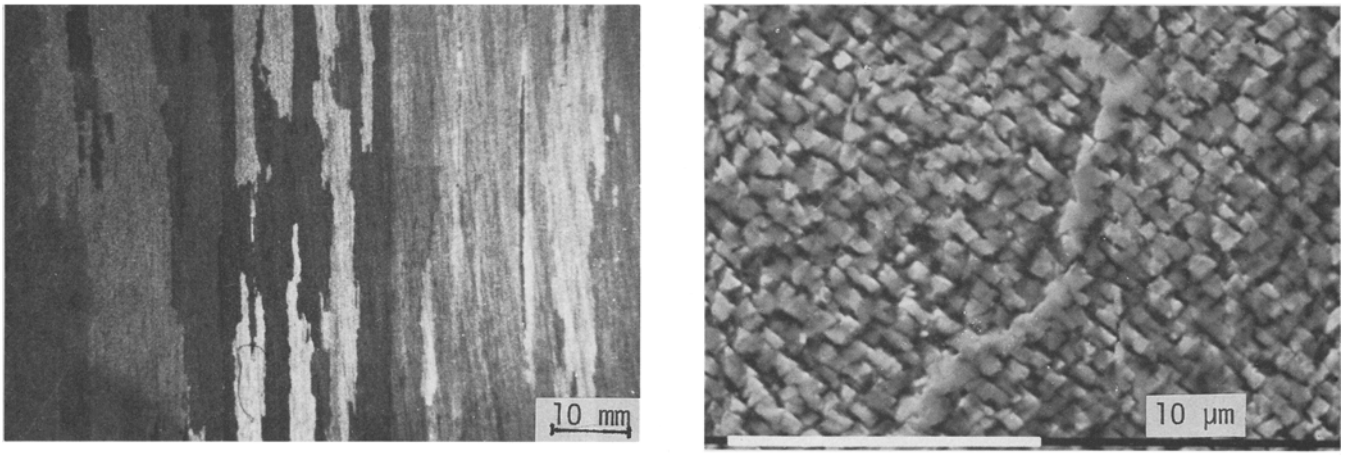

(a) (b)

Fig. 1 (a) Grain structure of MA 760. (b) Grain boundary covered with agglomerated γ'.

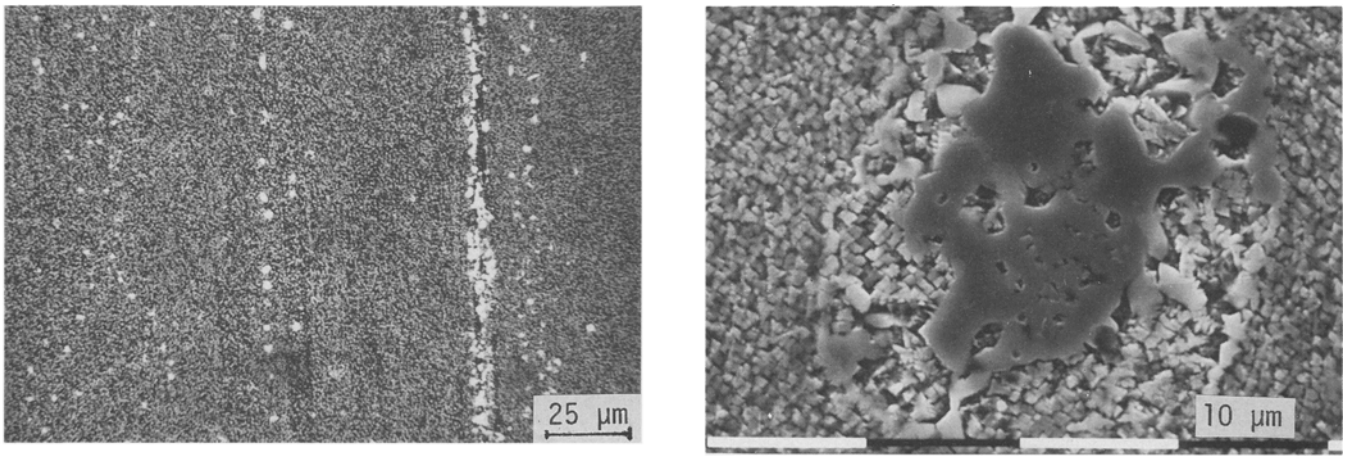

(a) (b)

Fig. 2 (a) Stringers of inclusions extending in the extrusion direction. (b) Typical inclusion with modified γ' structure surrounding it.

2. Experimental Procedure

The test material was a mechanically alloyed ODS nickel-base superalloy MA 760 delivered by Wiggin Alloys Ltd. Extruded bars with two different geometries having a small cross section (SCS) of 20 mm × 60 mm and a large cross section (LCS) of 32 mm × 95 mm were used. The final heat treatment, given by the supplier, was as follows: 0.5 h at 1120 °C, furnace cooled (FC) at 60 °C/min to 600 °C + FC. The compositions of the materials are given in Table 1.

Specimens for the LCF tests were cut from the SCS bar parallel to the extrusion direction (longitudinal direction, L) and from the LCS bar perpendicular to the extrusion direction (long transverse direction, LT). The gage sections of the samples were surface finished using SiC paper No. 1200. Fatigue tests were conducted using a closed loop mechanical materials testing machine and a high-temperature extensometer attached to the 12.5 mm longitudinal gage section. Samples were heated using a specially shaped induction coil, which resulted in the maximum measured temperature variation of ±5 °C within the gage length. All tests were performed in air under total strain control using triangular and symmetrical cycles ($R_\varepsilon = -1$), always starting in compression. The strain rate in all tests was $5 \times 10^{-3} s^{-1}$.

3. Results and Discussion

Because the microstructure of virgin MA 760 has not been documented extensively, a brief description is given below. The grain structure of MA 760 is very coarse, and the grains are elongated in the extrusion direction (Fig. 1a), the GAR being roughly 15. The texture in the extension direction is <110>, in

the long transverse direction <111>, and in the short transverse direction <112>. The γ' precipitates are nearly cuboidal, with the mean edge length of 0.50 μm. The volume fraction of γ' is close to 50%. The average dispersoid diameter is 30 nm, and the mean spacing between dispersoid particles is about 100 nm. The grain boundaries are primarily low-angle boundaries covered with agglomerated γ', as shown in Fig. 1(b). Stringers of inclusions extending in the extrusion direction, as well as separate inclusions, possibly nitrides, carbides or oxides, are commonly detected (Fig. 2a). The inclusions often change the chemical composition of the surrounding matrix and thereby the morphology of the γ' precipitates, as illustrated in Fig. 2(b). As a result of incomplete secondary recrystallization, small grains are sometimes observed.

The cyclic hardening curves presented in Fig. 3 show that the stress-strain response of MA 760 at constant-amplitude straining essentially does not change during cycling, although a small softening period at the beginning of the tests usually can be observed. Tests were conducted under total strain amplitude control, but because practically no hardening or softening took place, the plastic strain amplitudes presented in Table 2 can be considered to have remained constant during testing. At the end of the tests, the stress amplitude dropped suddenly, particularly in tests at 650 °C. This indicates that most of the fatigue life is used to initiate crack(s), which finally propagate very rapidly at the end of the test leading to failure of the specimen. When comparing the fatigue lives of L- and LT-samples, Table 2 shows that the fatigue lives in the L-direction are longer than in the LT-direction, as expected. When plotting fatigue lives as a function of the plastic strain amplitude, the fatigue lives at 650 °C are shorter than those at 900 or 950 °C. For the same amount of plastic deformation, however, much higher stresses are needed at 650 °C, which suggests that the crack initiation and early propagation are controlled by local effective stresses

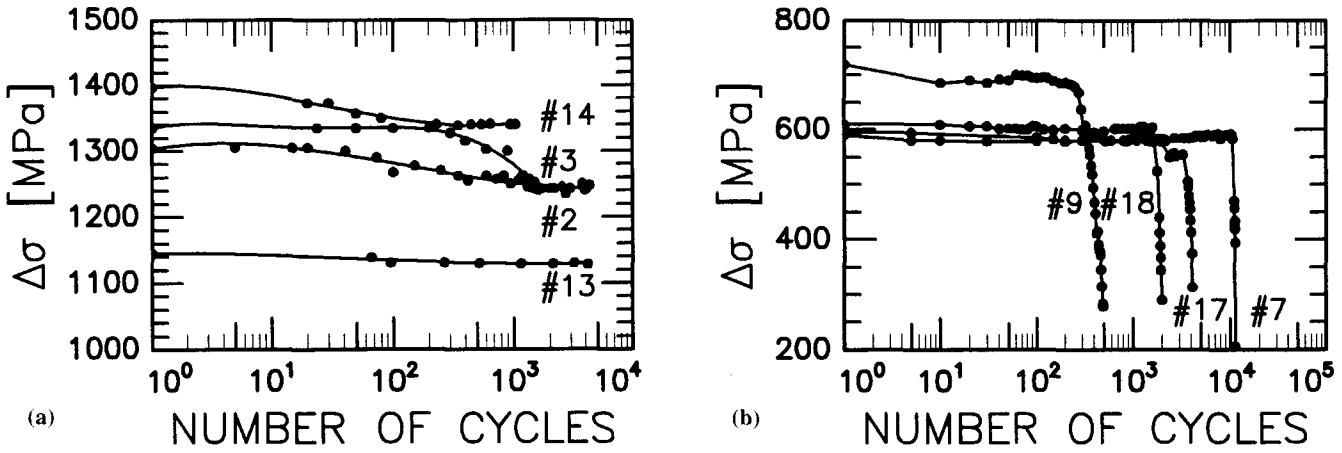

Fig. 3 Cyclic hardening curves at 650 °C (a), 900 and 950 °C (b). See Table 2 for test parameters.

Table 2 Results of low-cycle fatigue tests

Test No.	Orientation	Temperature, °C	Total strain range ($\Delta\varepsilon_t$), %	Plastic strain range ($\Delta\varepsilon_{pl}$), %	Elastic strain range ($\Delta\varepsilon_e$), %	Stress range ($\Delta\sigma$), MPa	Cycles to failure (N_f)
1	L	650	0.88	0.01	0.87	1225	12,480
2	L	650	0.93	0.02	0.91	1260	4,440
3	L	650	0.98	0.04	0.94	1330	1,642
4	L	650	1.14	0.05	1.09	1710	742
5	L	650	1.40	0.23	1.17	1789	283
6	L	900	0.38	0.02	0.36	412	21,903
7	L	900	0.56	0.02	0.54	588	11,280
8	L	900	0.71	0.17	0.54	628	1,079
9	L	900	0.83	0.20	0.63	700	492
10	L	900	1.34	0.57	0.77	880	198
11	L	900	1.93	1.11	0.82	852	117
12	L	900	2.42	1.50	0.92	948	49
13	LT	650	0.91	0.02	0.89	1145	5,034
14	LT	650	0.97	0.06	0.91	1360	1,192
15	LT	650	1.19	0.09	1.10	1610	636
16	LT	650	1.38	0.12	1.26	1625	98
17	LT	950	0.55	0.02	0.53	580	4,120
18	LT	950	0.61	0.04	0.57	600	2,021
19	LT	950	0.56	0.15	0.41	580	522
20	LT	950	1.04	0.33	0.71	850	112

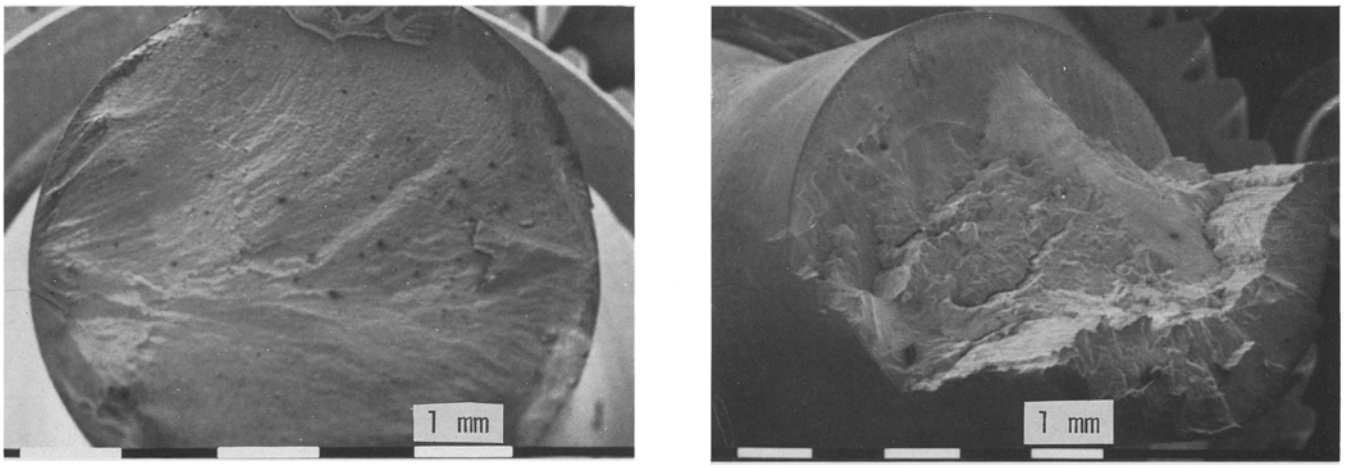

(a) (b)

Fig. 4 Fracture surfaces of MA 760. L-samples fatigued at (a) $\Delta\varepsilon_t = 0.98\%$, $T = 650$ °C and (b) $\Delta\varepsilon_t = 1.93\%$, $T = 900$ °C.

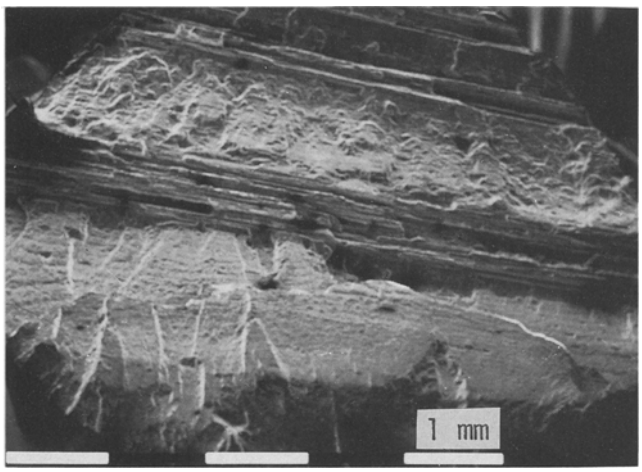

Fig. 5 Fracture surface of a MA 760 LT-sample fatigued at $\Delta\varepsilon_t = 1.04\%$, $T = 950$ °C.

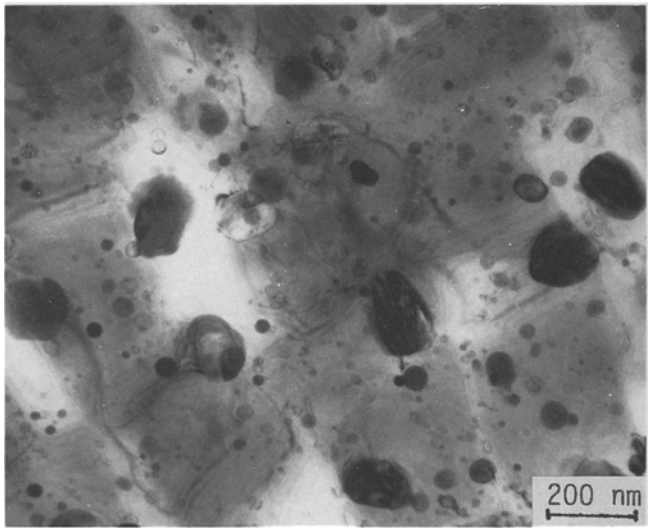

Fig. 6 Microstructure of as-received MA 760 sample cut perpendicular to the extrusion direction.

at the crack tip rather than by average plastic deformation. This type of behavior is also indicated by the increasing brittleness of the material with decreasing temperature.

The SEM studies of fracture surfaces revealed that the cracks nucleate at the specimen surface in a transgranular mode. In the fracture surface, two distinguishable areas can be observed—small areas with fatigue striations near the initiation point and an almost featureless area associated with the rapid crack growth. The amount of these smooth areas increases with decreasing temperature and increasing stress amplitude.

In the case of the L-samples, transgranular fracture dominates. However, at 900 °C, intergranular fracture propagating along axially oriented grain boundaries was occasionally observed in the rapid crack growth area. Two typical examples of fracture surfaces in the L-samples are presented in Fig. 4. In the LT-samples, the grains are elongated perpendicular to the loading axis, and intergranular fracture (Fig. 5) is more common, which may explain the reduction in fatigue lives compared to those of the L-samples.

The fatigued samples did not exhibit any extensive internal damage, such as voids and nonpropagating cracks, apart from localized damage in unrecrystallized regions or at inclusions. These were, however, also nonpropagating and did not affect the fracture behavior. Extensive secondary cracking along grain boundaries across the path of the primary crack was observed in all fatigued samples. It was noticed that cavitation-type damage on grain boundaries did not develop, and therefore, it was likely that the secondary cracking was due to oxidation. At these fairly slow test frequencies, when the crack tip arrives at a grain boundary, there will be time for oxygen diffusion to occur along the grain boundary. On subsequent strain cycles, a secondary crack will nucleate along the boundary and

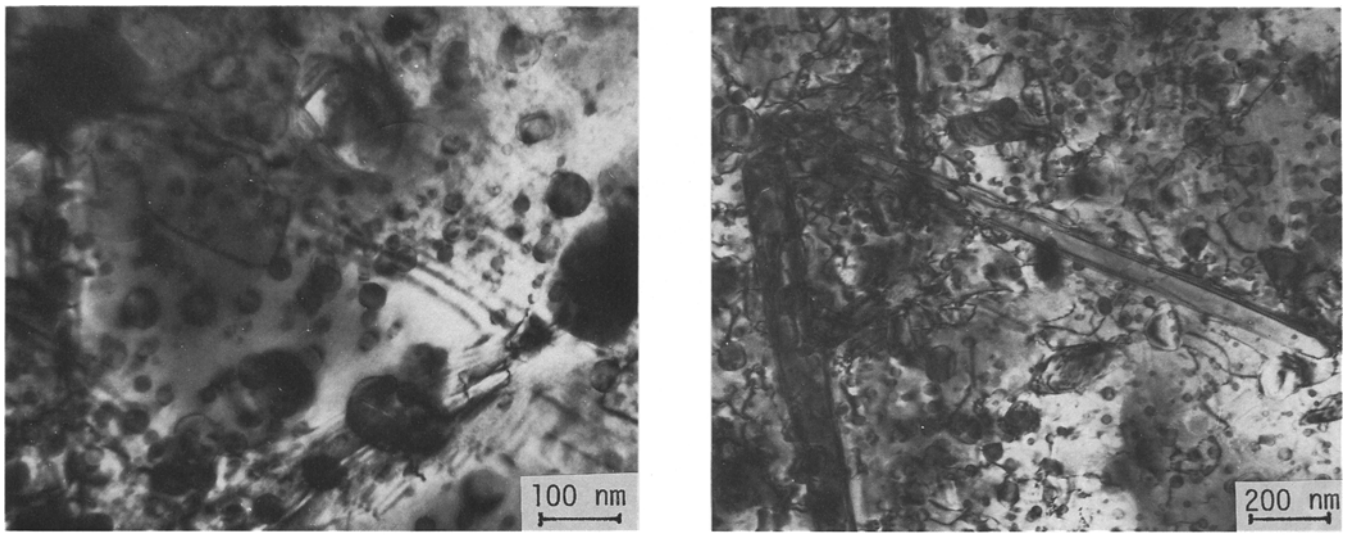

(a) (b)

Fig. 7 Microstructures of fatigued MA 760. TEM samples cut parallel to the fatigue specimen. (a) LT-sample, $\Delta\varepsilon_t = 0.91\%$, $T = 650$ °C. (b) L-sample, $\Delta\varepsilon_t = 0.56\%$, $T = 900$ °C.

then propagate by a combination of further oxidation and mechanical tearing.[6]

Dislocations in the fatigued specimens did not generally form any distinct arrangements normally observed in fatigued metallic materials. The amount of individual dislocations varied as a function of strain amplitude, but no cell formation was observed. As a function of increasing temperature and fatigue time, the γ' precipitates became bigger and more rounded, which is usually referred to as Ostwald ripening. Particularly at 650 °C, but also occasionally at higher temperatures, paired dislocations, which are indications of γ' cutting, were observed.[7] At 900 and 950 °C, dislocations commonly surrounded the γ' precipitates, pointing to the by-passing mechanism of γ'. Also, the lack of hardening and the saturation of the cyclic stress amplitude observed point to the existence of a dislocation by-passing mechanism.[8]

Dislocation climb over yttria particles was detected at all test temperatures. Dislocations were often pinned to the departure sides of Y_2O_3 particles and curved in areas between them. Departure side pinning is explained by the attractive interaction between the dislocations and the interface of incoherent particles, and it appears to be a common strengthening mechanism in ODS superalloys.[9] Figure 6 illustrates the microstructure of undeformed MA 760, and Fig. 7(a) and (b) are typical microstructures after cyclic straining at 650 and 900 °C.

References

1. G.W. Meethan, Superalloys in Gas Turbine Engines, *Met. Mater. Tech.*, Vol 14, 1982, p 387-392
2. J.S. Benjamin, Mechanical Alloying, *Sci. Am.*, Vol 5, 1976, p 40-48
3. Y. Kaieda, Trends in Development of Oxide-Dispersion-Strengthened Superalloys, *Trans. Nat. Res. Inst. Met.*, Vol 28(No. 3), 1986, p 18-24
4. M.J. Fleetwood, Mechanical Alloying—The Development of Strong Alloys, *Mater. Sci. Tech.*, Vol 2, 1986, p 1176-1182
5. H. Zeizinger and E. Arzt, The Role of Grain Boundaries in High Temperature Creep Fracture of an Oxide Dispersion Strengthened Superalloy, *Z. Metallkunde*, Vol 79, 1988, p 774-781
6. A. Tekin and J.W. Martin, Fatigue Crack Growth Behaviour of MA 6000, *Mater. Sci. Eng.*, Vol 96, 1987, p 41-49
7. E. Nembach and G. Neite, Precipitation Hardening of Superalloys by Ordered γ'-Particles, *Prog. Mater. Sci.*, Vol 29, 1985, p 177-319
8. J. Bressers and E. Arzt, High Temperature Low Cycle Fatigue of Inconel MA 6000, *High Temperature Alloys for Gas Turbines and Other Applications 1986*, W. Betz et al., Ed., Liége, Belgium, 1986, p 1067-1080
9. E. Arzt and S.D. Wilkinson, Threshold Stresses for Dislocation Climb over Hard Particles: The Effect of an Attractive Interaction, *Acta Metall.*, Vol 34, 1986, p 1893-1898